AEM
Journals.ASM.org

Novel Tripartite Aromatic Acid Transporter Essential for Terephthalate Uptake in *Comamonas* sp. Strain E6

Masaru Hosaka, Naofumi Kamimura, Shotaro Toribami, Kosuke Mori, Daisuke Kasai, Masao Fukuda, Eiji Masai

Department of Bioengineering, Nagaoka University of Technology, Nagaoka, Niigata, Japan

It has been suggested that a novel type of aromatic acid transporter, which is similar to the tripartite tricarboxylate transporter (TTT), is involved in terephthalate (TPA) uptake by *Comamonas* sp. strain E6. This suggestion was based on the presence of the putative TPA-binding protein gene, *tphC*, in the TPA catabolic operon. The *tphC* gene is essential for growth on TPA and is similar to the genes encoding TTT-like substrate-binding proteins. Here we identified two sets of E6 genes, *tctBA* and *tpiBA*, which encode TTT-like cytoplasmic transmembrane proteins. Disruption of *tctA* showed no influence on TPA uptake but resulted in a complete loss of the uptake of citrate. This loss suggests that *tctA* is involved in citrate uptake. On the other hand, disruption of *tpiA* or *tpiB* demonstrated that both genes are essential for TPA uptake. Only when both *tphC* and *tpiBA* were introduced with the TPA catabolic genes into cells of a non-TPA-degrading *Pseudomonas* strain did the resting cells of the transformant acquire the ability to convert TPA. From all these results, it was concluded that the TPA uptake system consists of the TpiA-TpiB membrane components and TPA-binding TphC. Interestingly, not only was the *tpiA* mutant of E6 unable to grow on TPA or isophthalate, it also showed significant growth delays on *o*-phthalate and protocatechuate. These results suggested that the TpiA-TpiB membrane components are able to interact with multiple substrate-binding proteins. The *tpiBA* genes were constitutively transcribed as a single operon in E6 cells, whereas the transcription of *tphC* was positively regulated by TphR. TPA uptake by E6 cells was completely inhibited by a protonophore, carbonyl cyanide *m*-chlorophenyl hydrazone, indicating that the TPA uptake system requires a proton motive force.

The uptake of substrates into cells is the first important cellular event in the assimilation of aromatic acids for bacteria. To date, various types of transporters involved in the uptake of aromatic acids have been characterized. The major facilitator superfamily (MFS) of transporters, which has 12 transmembrane α-helical spanners (TMSs), is the largest superfamily of secondary transporters (1). The aromatic acid/H^+ symporter (AAHS) family within MFS has been extensively characterized for the following: PcaK of *Pseudomonas putida* PRS2000 for the uptake of protocatechuate (PCA) and 4-hydroxybenzoate (2), TfdK of *Cupriavidus necator* JMP134 for 2,4-dichlorophenoxy acetate uptake (3), BenK of *Acinetobacter baylyi* ADP1 for benzoate uptake (4), GenK of *Corynebacterium glutamicum* ATCC 13032 for gentisate uptake (5), and MhbT of *Klebsiella pneumoniae* M5a1 for 3-hydroxybenzoate uptake (6).

On the other hand, only a limited number of studies characterized the substrate-binding protein (SBP)-dependent uptake systems, such as the ATP-binding cassette (ABC) transporters and the tripartite ATP-independent periplasmic transporters (TRAP-T), involved in the uptake of aromatic acids. The ABC transporters, primary active transporters driven by direct ATP hydrolysis, consist of an SBP, an integral membrane protein, and an ABC protein (7). Recent studies genetically demonstrated that ABC transporters are involved in the uptake of *o*-phthalate (OPA) both in *Burkholderia* strains (8) and *Rhodococcus jostii* RHA1 (9). The involvement of ABC transport systems was also suggested in the uptake of homogentisate by *P. putida* U (10), 2-chlorobenzoate by *Pseudomonas huttiensis* D1 (11), 4-hydroxybenzoate by *Acinetobacter* sp. strain BEM2 (12), and 4-hydroxyphenylacetate by *Klebsiella pneumoniae* M5a1 (13).

The two known families of SBP-dependent secondary transporters are TRAP-T (14) and the tripartite tricarboxylate transporters (TTT) (15). These two families of transporters have similar tripartite structures, which consist of an SBP and two transmembrane proteins of different sizes. However, both transporters are not related to each other at the amino acid sequence level. An example of the TRAP-T involved in the uptake of aromatic acids has been reported only for the *fcbT1T2T3* genes encoding the 4-chlorobenzoate transporter of *Comamonas* sp. strain DJ-12 (16). In contrast, there have been no reports on TTT-like aromatic acid transporters. The prototype of TTT is the TctCBA system, encoded by the *tctCBA* operon of *Salmonella enterica* serovar Typhimurium (17–19). This prototype mediates the uptake of citrate and comprises a large transmembrane protein, TctA (504 amino acids [aa]), with 12 predicted TMSs, a small transmembrane protein, TctB (144 aa), with four putative TMSs, and a periplasmic citrate-binding protein TctC (325 aa). A decade ago, 78 genes predicted to encode periplasmic solute receptors (Bug receptors) were found in *Bordetella pertussis* (20). In this large number of Bug receptor genes, *bctC* (formerly *bug4*) in the *bctCBA* operon was characterized as encoding a citrate-binding protein (20, 21). The X-ray crystal structure of one of the Bug receptors of unknown function, BugD (formerly Bug74), was determined. It was suggested that BugD is an aspartate receptor (22). Since the specific ligand-binding motif of BugD was highly conserved in the Bug receptors, these proteins were considered receptors of amino acids or other carboxylated solutes. In addition, large numbers of

Received 5 June 2013 Accepted 26 July 2013
Published ahead of print 2 August 2013
Address correspondence to Eiji Masai, emasai@vos.nagaokaut.ac.jp.
Supplemental material for this article may be found at http://dx.doi.org/10.1128/AEM.01600-13.

doi:10.1128/AEM.01600-13

bug homologs were also found in the genomes of *Bordetella bronchiseptica* (181 *bug* homologs), *Bordetella parapertussis* (143 *bug* homologs), and *Cupriavidus metallidurans* (102 *bug* homologs) even though the genomes of these species and of *B. pertussis* have only between two and five membrane component gene homologs (*tctBA* homologs) each (20). These observations suggest that a number of SBPs play roles in the uptake of various solutes through their interaction with a limited number of membrane components.

In our previous studies, we characterized the two similar terephthalate (TPA) catabolic operons, $tphR_I$-$tphC_IA2_IA3_IB_IA1_I$ and $tphR_{II}$-$tphC_{II}A2_{II}A3_{II}B_{II}A1_{II}$ (23), and the isophthalate (IPA) catabolic operon *iphACBDR* (24) in a phthalate isomer-degrading bacterium, *Comamonas* sp. strain E6. Interestingly, the *tph* and *iph* operons contain *tphC* and *iphC*, respectively, whose products showed 35% identity at the amino acid sequence level to the product of one of the *bug* receptor genes, *bugT* (*bug1*) of *B. pertussis* (25). An introduction of a plasmid carrying $tphR_{II}$-$tphC_{II}A2_{II}A3_{II}B_{II}A1_{II}$ conferred the TPA utilization phenotype on *Comamonas testosteroni* IAM 1152, which is able to grow on PCA but not on TPA (23). The presence of *tphC* was essential for this phenotype. Similarly, *iphC* was required for the growth of E6 on IPA (24). All these facts implied that *tphC* and *iphC* encode a TPA-binding protein and an IPA-binding protein, respectively, and that these SBPs interact with unidentified membrane components to take up the substrates.

In this study, we identified and characterized the two gene sets, both of which encode a small transmembrane protein and a large transmembrane protein, involved in the uptake of citrate and TPA.

MATERIALS AND METHODS

Bacterial strains, plasmids, and culture conditions. The bacterial strains and plasmids used in this study are listed in Table S1 in the supplemental material. *Comamonas* sp. strain E6 was grown in lysogeny broth (LB; 10 g/liter Bacto tryptone, 5 g/liter yeast extract, and 5 g/liter NaCl) or in Wx minimal salt medium (26) containing 10 mM TPA or 10 mM succinate at 30°C. *Pseudomonas putida* PpY1100 was grown in LB at 30°C. *Escherichia coli* strains were grown in LB at 37°C. For cultures of cells carrying antibiotic resistance markers, the media for *E. coli* transformants were supplemented with 100 mg of ampicillin (Ap)/liter, 25 mg of kanamycin (Km)/liter, and 12.5 mg of tetracycline (Tc)/liter. The media for PpY1100 transformants were supplemented with 25 mg of Tc/liter, and the media for E6 transformants and mutants were supplemented with 12.5 mg Tc/liter and 50 mg Km/liter, respectively.

Uptake assays. E6 and its mutant cells were grown in Wx medium containing 10 mM succinate for 12 h. Cells were harvested by centrifugation at 5,000 × *g* for 10 min and washed twice with Wx medium. The resultant cells were inoculated into Wx medium containing 10 mM succinate or 10 mM succinate plus 10 mM TPA to an optical density at 600 nm (OD_{600}) of 0.2 and incubated for 4 h. After the incubation, cells were collected by centrifugation, washed twice with 50 mM Tris-morpholineethanesulfonic acid (Tris-MES) buffer (pH 7.5; buffer A), and resuspended in the same buffer to an OD_{600} of 20. TPA uptake was measured at 30°C in a total volume of 650 μl mixture, which contained the cells suspended in buffer A to an OD_{600} of 2.0 and 20 μM [carboxy-^{14}C]TPA (60 mCi/mmol; American Radiolabeled Chemicals Inc.). Uptake was started by adding the substrate to the cell suspension. The 100-μl samples were collected from the reaction mixture at 10 s, 30 s, 1.0 min, 2.0 min, and 3.0 min and filtrated through nitrocellulose membranes (0.45 μm pore size; Advantec, Tokyo, Japan). After the filtrates were washed with 1 ml of buffer A three times, accumulated TPA inside the cells was determined by scintillation counting (AccuFLEX LSC-7400; Aloca Co. Ltd., Tokyo, Japan). The uptake rate was calculated at time points 10 and 60 s and expressed as the amount of substrates transported into the cells in 1 min per 1 mg of cellular proteins at 30°C. Each experiment was triplicated, and data were averaged with standard deviations. The protein concentration was determined using a DC protein assay kit (Bio-Rad, Hercules, CA).

By using 50 mM Tris-MES buffer, the optimal pH for TPA uptake was determined, with pH ranging from 5.5 to 9.5. An inhibition experiment using carbonyl cyanide *m*-chlorophenyl hydrazone (CCCP) was performed by incubation of the cell suspensions with 100 μM CCCP for 5 min at 30°C prior to adding the substrate. The effect of the presence of aromatic acids on TPA uptake was examined by adding 2 mM TPA, IPA, OPA, benzoate, 3-hydroxybenzoate, 4-hydroxybenzoate, PCA, vanillate, or syringate to the reaction mixture containing 20 μM [^{14}C]TPA and cells.

For citrate uptake measurement, E6 and its mutant cells grown with succinate were inoculated into Wx medium containing 10 mM succinate or 10 mM succinate plus 10 mM citrate to an OD_{600} of 0.2 and incubated for 4 h. Utilizing these cells, citrate uptake was measured using 20 μM [1,5-^{14}C]citrate (55 mCi/mmol; American Radiolabeled Chemicals Inc.).

Cloning of the genes. Degenerate primers for amplification of a *tctA* homolog in E6, TCTF and TCTR, were designed based on the sequences of *tctA* homologs in *C. testosteroni* KF-1 (CtesDRAFT_PD3800), *Delftia acidovorans* SPH-1 (Daci_2520), and *Acidovorax* sp. strain JS42 (Ajs_1644). A second primer set, 4157F and 4157R, was used for the amplification of another *tctA* homolog found in KF-1 (CtesDRAFT_PD4157). Nucleotide sequences of these primers are shown in Table S2 in the supplemental material. A 405-bp fragment and a 452-bp fragment were PCR amplified using primer sets TCTF-TCTR and 4157F-4157R, respectively. Their nucleotide sequences were then determined using a CEQ2000XL genetic analysis system (Beckman Coulter Inc., Fullerton, CA). The PCR-amplified fragments were used in colony hybridization as probes to isolate the EcoRI fragments carrying *tctA* homologs from the E6 gene library, constructed in Charomid 9-36, containing EcoRI digests of the E6 total DNA. Colony and Southern hybridization analyses were done using the digoxigenin (DIG) system (Roche, Mannheim, Germany). Deletion clones were constructed with the 6.1-kb EcoRV-EcoRI region carrying the 405-bp amplicon and the 4.6-kb EcoRV-EcoRI region carrying the 452-bp amplicon, and their nucleotide sequences were determined. Sequence analysis was performed using the MacVector program (MacVector, Inc., Cary, NC). Homology searches were carried out with the nonredundant (nr) protein sequence database using the BLAST program. A pairwise alignment was performed with the EMBOSS alignment tool at http://www.ebi.ac.uk/Tools/psa/emboss_needle/. Putative TMSs were predicted using the TMHMM (27), TopPred II (28), and SOSUI (29) programs.

Construction of mutants. Construction of p18TAK, pK19tAIIK, and pK18tBK for disruption of *tctA*, *tpiA*, and *tpiB*, respectively, is described in the supplemental material. To obtain *tctA*, *tpiA*, and *tpiB* mutants, p18TAK, pK19tAIIK, and pK18tBK were independently introduced into E6 cells by electroporation and candidate mutants were isolated as described previously (30). The disruption of each gene was examined by Southern hybridization analysis (see Fig. S1 in the supplemental material).

E6 mutant cells were pregrown in 10 ml of LB containing Km. The cells were harvested by centrifugation at 5,000 × *g* for 10 min, washed twice with Wx medium, and resuspended with 3 ml of the same medium. The cells were inoculated into Wx medium containing 10 mM TPA, IPA, OPA, PCA, or citrate to an OD_{600} of 0.1. Cell growth was periodically monitored by measuring OD_{600}. Complementary plasmids pJBtpiA carrying *tpiA* and pJBtpiB carrying *tpiB*, constructed using pJB866, were independently introduced into cells of EME019 and EME020, respectively, by electroporation, and the growth of the resulting transformant cells was examined.

Reverse transcription-PCR (RT-PCR) and quantitative RT-PCR (qRT-PCR). E6 cells grown in LB were washed twice with Wx medium and resuspended in the same medium containing 10 mM succinate with or without 10 mM TPA to an OD_{600} of 0.2. The cells were then incubated for 4 h at 30°C. Total RNA was isolated using Isogen II (Nippon Gene, Tokyo, Japan), followed by treatment with RNase-free DNase I (Roche).

Single-strand cDNA was synthesized from 2 μg of total RNA utilizing PrimeScript reverse transcriptase (TaKaRa Bio Inc., Otsu, Japan) with random hexamer primers. PCR was performed with the cDNA mixture, specific primers (see Table S2 in the supplemental material), and PrimeStar GXL DNA polymerase (TaKaRa Bio Inc.).

A qRT-PCR analysis was carried out using a Fast SYBR green master mix (Applied Biosystems, Foster City, CA) with a StepOne real-time PCR system (Applied Biosystems) according to previously reported methods (31). Primers used for real-time PCR are listed on Table S2 in the supplemental material. To normalize the amount of RNA in each sample, 16S rRNA was used as an internal standard.

Expression of *tpiBA* and *tphC*$_{II}$ with *tphA2*$_{II}$*A3*$_{II}$*B*$_{II}$*A1*$_{II}$ in *P. putida*. The pJB866-based plasmids pJBA, pJC, and pJCBA, which carry *tpiBA*, *tphC*$_{II}$, and *tphC*$_{II}$-*tpiBA*, respectively, under the control of the P$_m$ promoter, were constructed. To obtain pJB866-based plasmids expressing *tpiBA*, *tphC*$_{II}$, or *tphC*$_{II}$-*tpiBA* with *tphA2*$_{II}$*A3*$_{II}$*B*$_{II}$*A1*$_{II}$, the DNA fragments, which contain *tpiBA*, *tphC*$_{II}$, or *tphC*$_{II}$-*tpiBA* with the P$_m$ promoter and *xylS*, encoding a transcriptional regulator for expression from the P$_m$ promoter, were ligated into pJSK63 carrying *tphA2*$_{II}$*A3*$_{II}$*B*$_{II}$*A1*$_{II}$ under the control of the P$_m$ promoter. The plasmids pJBAtG, pJCtG, and pJCBAtG, carrying *tpiBA*, *tphC*$_{II}$, and *tphC*$_{II}$-*tpiBA*, respectively, with *tphA2*$_{II}$*A3*$_{II}$*B*$_{II}$*A1*$_{II}$ were constructed. The details of plasmid construction are described in the supplemental material.

The plasmids pJCBA, pJBAtG, pJCtG, and pJCBAtG were introduced into the cells of *P. putida* PpY1100 by electroporation, and then the resulting transformant cells were pregrown in LB containing Tc. The cells were grown in fresh LB containing Tc and 1 mM *m*-toluate, which is an inducer of expression from the P$_m$ promoter, for 10 h at 30°C. The cells were harvested by centrifugation at 5,000 × *g* for 5 min, washed three times with 50 mM Tris-HCl buffer (pH 7.5), and resuspended in the same buffer. Cells suspended in the buffer were sonicated, and the cell lysate was centrifuged at 19,000 × *g* for 15 min to obtain cell extracts. Conversions of TPA by the cell extracts of transformants were examined in a 1-ml reaction mixture containing 150 μM TPA, 200 μM NADPH, cell extract (500 μg of protein), and 50 mM Tris-HCl buffer (pH 7.5). Portions of the reaction mixtures were periodically removed, and the reaction was stopped by the addition of HCl. The remaining TPA was extracted with ethyl acetate, dissolved in 25% acetonitrile in water, filtrated, and analyzed by high-performance liquid chromatography (HPLC; Acquity UPLC system; Waters, Milford, CT) coupled to electrospray ionization-mass spectrometry (ESI-MS; Acquity TQ detector; Waters). HPLC separation was achieved using a TSKgel ODS-140HTP column (2.0 by 100 mm; Tosoh, Tokyo, Japan). The mobile phase of the HPLC system was a mixture of water (75%) and acetonitrile (25%) containing 0.1% formic acid at a flow rate of 0.3 ml/min. TPA and its metabolite PCA were detected at 242 nm. In the ESI-MS analysis, mass spectra were obtained using the negative ion mode with the settings specified in a previous study (31). Conversions of TPA by the resting cells of transformants were examined in a 0.5-ml reaction mixture containing 1 mM TPA, cells with an OD_{600} of 20, and 50 mM Tris-HCl buffer (pH 7.5). The reaction mixtures were incubated with shaking for 60 min at 30°C. Portions of the mixtures (20 μl) were periodically collected, and the cells were removed by centrifugation. The supernatants were then diluted 5-fold in water, filtrated, and analyzed by HPLC as described above.

Nucleotide sequence accession numbers. The nucleotide sequences reported in this paper were deposited in the DDBJ, EMBL, and GenBank nucleotide sequence databases under accession numbers AB822590 and AB822591.

RESULTS

Characterization of TPA uptake by *Comamonas* sp. E6 cells. Uptake of TPA by *Comamonas* sp. strain E6 cells grown in Wx medium containing 10 mM succinate or 10 mM succinate plus 10 mM TPA was examined using [^{14}C]TPA. Cells suspended to an OD_{600} of 2.0 in 50 mM Tris-MES buffer (pH 7.5) were incubated with 20 μM [^{14}C]TPA, and the amount of [^{14}C]TPA incorporated into the cells was periodically measured. As shown in Fig. 1A, only the cells grown on TPA showed the uptake of TPA. This result indicated that the transcription of at least a part of the component genes for the TPA transporter was induced during the growth on TPA. When the TPA uptake rate was determined at pHs between 5.5 and 9.5, the maximum uptake rate was observed at pH 7.5 (2.55 ± 0.88 nmol/mg of protein · min). At pH 5.5, the uptake rate was approximately 10% of that at pH 7.5, and TPA uptake was not seen at pH 9.0 and 9.5.

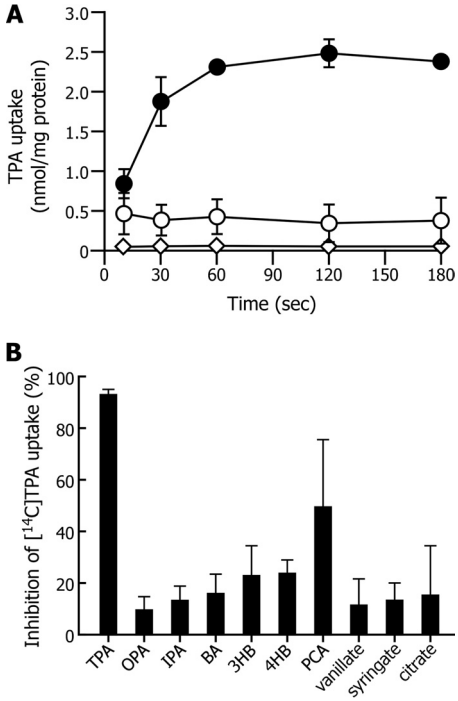

FIG 1 Uptake of [^{14}C]TPA by cells of *Comamonas* sp. strain E6. (A) [^{14}C]TPA uptake by E6 cells grown in the presence and absence of TPA is indicated by solid circles and open circles, respectively. [^{14}C]TPA uptake by TPA-induced E6 cells treated with 100 μM CCCP is indicated by diamonds. Each value is the average ± standard deviation of three independent experiments. (B) Substrate inhibition of TPA uptake. The uptake rates of TPA were examined by adding 2 mM aromatic acids or citrate as competitors to the reaction mixture containing 20 μM [^{14}C]TPA. The TPA uptake rate in the absence of competitors was 2.62 ± 0.38 nmol/mg of protein · min. Inhibition was evaluated by comparing the TPA uptake rates in the presence and absence of competitors. Each value is the average ± standard deviation of three independent experiments. BA, benzoate; 3HB, 3-hydroxybenzoate; 4HB, 4-hydroxybenzoate.

In order to determine the energy dependence of TPA transport, inhibition of TPA uptake was assessed using E6 cells treated with protonophore CCCP. CCCP completely inhibited TPA uptake (Fig. 1A); therefore, the transport of TPA into E6 cells was found to be dependent on a proton motive force.

TPA uptake rates were examined in the presence of other aromatic acids (OPA, IPA, benzoate, 3-hydroxybenzoate, 4-hydroxybenzoate, PCA, vanillate, or syringate) or citrate as competitors (Fig. 1B). When 2 mM unlabeled TPA was used as a competitor, the uptake rate of 20 μM [^{14}C]TPA by E6 cells was reduced to 6.7% of the rate in the absence of a competitor. Among other compounds, the addition of PCA resulted in a significant decrease in the TPA uptake rate (approximately 50% of the rate in the absence of PCA).

Isolation of the genes encoding TTT-like transmembrane proteins. In order to isolate the *Comamonas* sp. strain E6 genes that encode predicted transmembrane proteins of the TPA transporter, we searched the *Comamonas testosteroni* KF-1 genome for *tctA* homologs, which are similar to the gene encoding the large transmembrane protein of the citrate transporter of *S.* Typhimurium. Since *C. testosteroni* KF-1 carries almost the same *tphCA2A3BA1* gene set as E6, KF-1 was expected to have the genes encoding TTT-like transmembrane proteins involved in TPA uptake. A database search revealed the presence of two open reading frames (ORFs), CtesDRAFT_PD3800 and CtesDRAFT_PD4157, of unknown functions, both of which encoded products having 39% identity with the deduced amino acid sequence of the product of *tctA* of *S.* Typhimurium. CtesDRAFT_PD3802 and CtesDRAFT_PD3801, upstream of CtesDRAFT_PD3800, showed similarities with *tctC* and *tctB*, encoding the citrate-binding protein and the small transmembrane protein of *S.* Typhimurium, respectively. In the case of CtesDRAFT_PD4157, only the *tctB* ortholog (CtesDRAFT_PD4158), which encoded a product having 18% identity with *S.* Typhimurium TctB, was found just upstream of CtesDRAFT_PD4157. Since gene sets similar to CtesDRAFT_PD3800-3802 were also found in the genomes of *Delftia acidovorans* SPH-1 and *Acidovorax* sp. strain JS42, we designed a primer pair to amplify a partial sequence of a CtesDRAFT_PD3800 ortholog of E6 on the basis of the highly conserved sequences between KF-1, SPH-1, and JS42. Primers used for the amplification of a CtesDRAFT_PD4157 ortholog were designed using the KF-1 sequences. With these primer pairs, 405-bp and 452-bp fragments (fragments A and B) were amplified from E6 total DNA by PCR. Nucleotide sequences of fragments A and B showed 92.6% and 93.4% identities with the same regions of CtesDRAFT_PD3800 and CtesDRAFT_PD4157, respectively. This suggested that E6 has gene sets similar to CtesDRAFT_PD3800 and CtesDRAFT_PD4157. In order to isolate these presumed gene sets, the E6 Charomid libraries were screened by colony hybridization using fragments A and B as probes. Then 8.9-kb and 7.6-kb EcoRI fragments containing fragments A and B were isolated. The nucleotide sequence of the 6,106-bp EcoRV-EcoRI region in the 8.9-kb EcoRI fragment revealed the presence of six ORFs highly homologous to CtesDRAFT_PD3804-PD3799 (89.3 to 99.1% identities) (Fig. 2A). Based on the similarities to the citrate transporter of *S.* Typhimurium, we gave the ORFs homologous to CtesDRAFT_PD3802, CtesDRAFT_PD3801, and CtesDRAFT_PD3800 the designations *tctC*, *tctB*, and *tctA*, respectively. Upstream of E6 *tctC*, there are two divergently transcribed ORFs that encode a putative histidine kinase (*tctE*) and a response regulator (*tctD*); these ORFs are similar to CtesDRAFT_PD3804 and CtesDRAFT_PD3803, respectively. On the other hand, the nucleotide sequence of the 4,567-bp EcoRV-EcoRI region in the 7.6-kb EcoRI fragment showed the presence of four ORFs highly similar to CtesDRAFT_PD4159-PD4156 (94.4 to 98.7% identities; Fig. 2B). The ORFs similar to CtesDRAFT_PD4158 and CtesDRAFT_PD4157, which appeared to encode small and large transmembrane proteins, respectively, were designated *tpiB* and *tpiA*. In the vicinity of *tpiBA*, SBP gene-like genes were not found.

Characterization of the *tctA* mutant. To examine the function of *tctA*, *tctA* in *Comamonas* sp. strain E6 was disrupted by the insertion of the Km resistance gene (see Fig. S1 in the supplemental material). The resulting mutant, EME018, grew on TPA similarly to the wild type (see Fig. S2). The rate of uptake of [^{14}C]TPA by EME018 cells grown on TPA was almost the same as that by the wild type (Fig. 3A). On the other hand, EME018 cells were unable

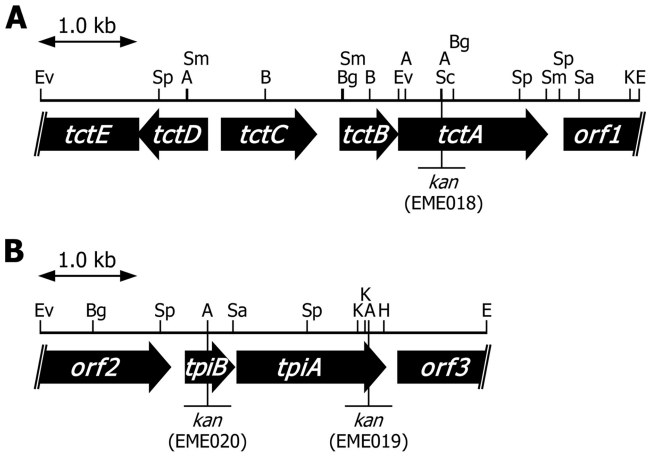

FIG 2 Restriction maps of the 6.1-kb EcoRV-EcoRI fragment carrying *tctCBA* (A) and the 4.6-kb EcoRV-EcoRI fragment carrying *tpiBA* (B). Vertical bars indicate the positions of the *kan* gene insertion in the *tctA* mutant (EME018), *tpiB* mutant (EME020), and *tpiA* mutant (EME019). Abbreviations for restriction enzymes: A, ApaI; B, BamHI; Bg, BglII; E, EcoRI; Ev, EcoRV; H, HindIII; K, KpnI; Sa, SalI; Sc, ScaI; Sm, SmaI; Sp, SphI.

to grow on citrate (Fig. 3B). In order to evaluate the ability of EME018 cells to take up citrate, uptake of [^{14}C]citrate by E6 cells was verified using cells grown on 10 mM succinate or 10 mM succinate plus 10 mM citrate. Since only the cells grown in the presence of citrate showed a significant uptake of citrate (Fig. 3C), the citrate uptake genes appeared to be expressed during the incubation of E6 cells on citrate. In contrast, the cells of EME018 grown in the presence of citrate had no citrate uptake activity (Fig. 3C). All these results strongly suggested that *tctA* is involved in the transport of citrate.

Characterization of *tpiA* and *tpiB* mutants. In order to examine the involvement of *tpiA* and *tpiB* in TPA uptake by *Comamonas* sp. strain E6, a *tpiA* mutant (EME019) and a *tpiB* mutant (EME020) were created by the insertion of the Km resistance gene into each gene (see Fig. S1 in the supplemental material). EME019 completely lost the ability to grow on TPA and IPA (Fig. 4A and B), suggesting that *tpiA* is involved in the uptake of these substrates. Introduction of pJBtpiA carrying *tpiA* into the EME019 cells partially restored the growth of the mutant on TPA and IPA (see Fig. S3). These results indicated that *tpiA* is indispensable for the growth of E6 on TPA and IPA. Similarly, EME020 lost the ability to grow on TPA and IPA, and the introduction of pJBtpiB carrying *tpiB* into the EME020 cells restored the growth of the mutant on TPA (see Fig. S4). These results indicate that *tpiB* is also involved in the growth of E6 on these substrates. Interestingly, the growth of EME019 on OPA, PCA, and citrate was significantly retarded (Fig. 4C to E). Similar growth defects on OPA and PCA were also observed for EME020 (see Fig. S4). These observations suggested that *tpiA* and *tpiB* contribute in part to the uptake of OPA, PCA, and citrate.

To confirm that the growth deficiency of EME019 on TPA was caused by the incapability of the mutant cells to take up TPA, [^{14}C]TPA uptake by EME019 cells grown on TPA was evaluated. EME019 cells showed no TPA uptake activity, while the introduction of pJBtpiA into EME019 cells restored the activity (Fig. 5A). In addition, the EME020 cells grown on TPA also exhibited no TPA uptake activity (Fig. 5B). These results indicated that *tpiA*

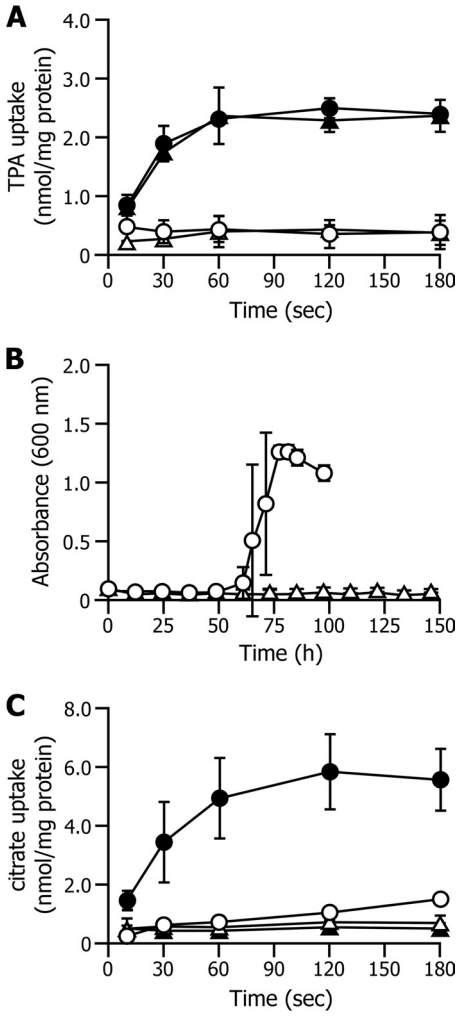

FIG 3 Characterization of the *tctA* mutant. (A) [^{14}C]TPA uptake assays were performed with E6 cells (circles) and *tctA* mutant cells (EME018; triangles) grown in the presence (solid symbols) or absence (open symbols) of TPA. (B) Growth of E6 cells (circles) and EME018 cells (triangles) on Wx medium containing 10 mM citrate. (C) [^{14}C]citrate uptake assays were performed with E6 cells (circles) and EME018 cells (triangles) grown in the presence (solid symbols) or absence (open symbols) of citrate. Each value is the average ± standard deviation of three independent experiments.

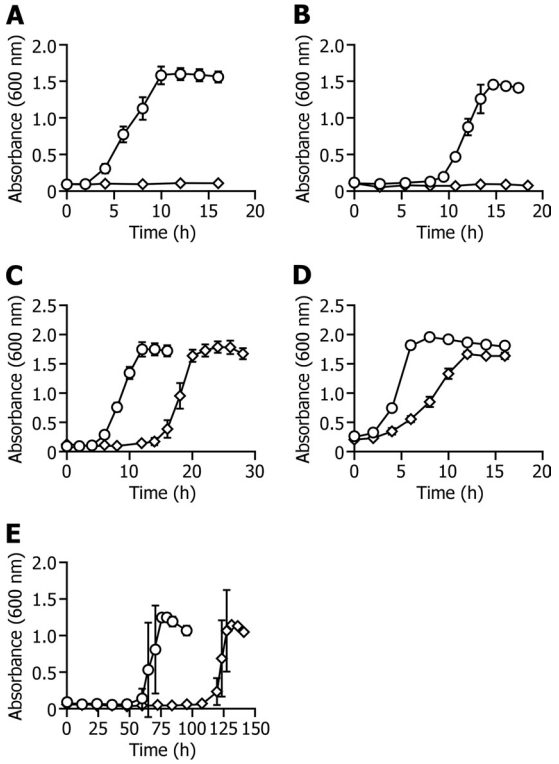

FIG 4 Growth of the *tpiA* mutant on various aromatic acids and citrate. E6 cells (circles) and *tpiA* mutant cells (EME019; diamonds) were incubated in Wx medium containing 10 mM TPA (A), IPA (B), OPA (C), PCA (D), or citrate (E). Each value is the average ± standard deviation of three independent experiments.

and *tpiB* are essential for the uptake of TPA and probably also IPA uptake. Since the growth of EME019 on citrate was considerably retarded, citrate uptake by EME019 cells grown in the presence of citrate was also assessed (Fig. 5C). The rate of uptake of [^{14}C]citrate by EME019 cells decreased to approximately 54% of the rate of uptake by the wild type.

Transcription of *tpiBA* and *tphC* in *Comamonas* sp. strain E6. RT-PCR analysis was performed to define the transcriptional unit of *tpiBA* using the total RNA isolated from E6 cells grown on TPA and primers amplifying the intergenic regions of neighboring ORFs. Amplifications of the internal regions of *tpiB* and *tpiA* and the intergenic region of *tpiB-tpiA* were observed, whereas the regions *orf2-tpiB* and *tpiA-orf3* showed no amplification (see Fig. S5 in the supplemental material). Therefore, it is concluded that *tpiBA* is transcribed in a single transcriptional unit. In a previous study, we reported that the transcription of *tphCA2A3BA1* is positively regulated by an IclR-type transcriptional regulator, TphR, in the presence of TPA. To examine whether *tpiBA* is inducibly expressed in E6, qRT-PCR analysis was performed using total RNA isolated from E6 cells grown in the presence or absence of TPA. This analysis showed that the transcription of *tphC* was induced approximately 21-fold in the cells grown in the presence of TPA (Fig. 6). On the other hand, the transcription levels of *tpiB* and *tpiA* in the cells grown with TPA were almost equal to those in the cells grown without TPA (Fig. 6). These results indicate that *tpiBA* is constitutively expressed in E6 cells.

Expression of $tphC_{II}$ and *tpiBA* with $tphA2_{II}A3_{II}B_{II}A1_{II}$ in *P. putida*. In a previous study, we observed that the introduction of pEJ89 carrying $tphR_{II}$-$tphC_{II}A2_{II}A3_{II}B_{II}A1_{II}$, conferred the TPA utilization phenotype on *C. testosteroni* IAM 1152, which is able to grow on PCA but not on TPA (23). In contrast, introduction of the same plasmid was not able to confer the ability to convert TPA on *P. putida* PpY1100, which is unable to grow on either PCA or TPA. These observations implied that PpY1100 was not able to take up TPA due to the lack of the *tpiBA* ortholog. Therefore, we examined whether the introduction of *tpiBA* could provide PpY1100 cells an ability to convert TPA. In these experiments, we first observed that the resting PpY1100 cells harboring pJCtG, which carries $tphC_{II}$ and $tphA2_{II}A3_{II}B_{II}A1_{II}$, were scarcely able to convert TPA (Fig. 7). Because the extract of the same cells converted TPA into PCA (see Fig. S6 in the supplemental material), this deficiency of TPA conversion appeared to be due to the inability of PpY1100 cells to take up TPA. On the other hand, no conversion was achieved by the cell extract of

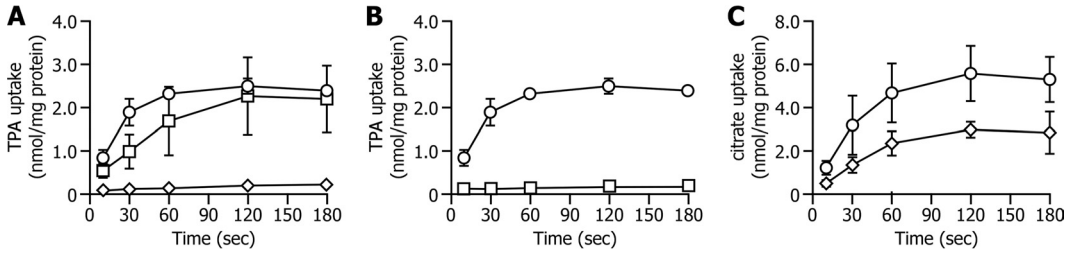

FIG 5 Characterization of *tpiA* and *tpiB* mutants. (A) [^{14}C]TPA uptake assays were performed with E6 cells (circles), *tpiA* mutant cells (EME019; diamonds), and EME019 cells harboring pJBtpiA (squares) grown in the presence of TPA. (B) [^{14}C]TPA uptake assays were performed with E6 cells (circles) and *tpiB* mutant cells (EME020; squares) grown in the presence of TPA. (C) [^{14}C]citrate uptake assays were performed with E6 cells (circles) and EME019 cells (diamonds). Each value is the average ± standard deviation of three independent experiments.

PpY1100 harboring pJCBA, which carries $tphC_{II}$ and *tpiBA* (see Fig. S6). The resting PpY1100 cells harboring pJBAtG, which carries *tpiBA* and $tphA2_{II}A3_{II}B_{II}A1_{II}$, showed no TPA-converting activity as well. However, the resting PpY1100 cells harboring pJCBAtG, which contains $tphC_{II}$, *tpiBA*, and $tphA2_{II}A3_{II}B_{II}A1_{II}$, showed the ability to transform TPA (Fig. 7). All the above results strongly support the conclusion that the TPA transporter of E6 consists of the TPA-binding TphC and the TpiA-TpiB transmembrane proteins.

DISCUSSION

We identified *tctBA* and *tpiBA* in *Comamonas* sp. strain E6, both of which encode TTT-like small and large transmembrane proteins (Fig. 2). The deduced amino acid sequences encoded by *tpiA* and *tpiB* showed 42.0% and 16.6% identities with those encoded by *tctA* and *tctB*, respectively. The similarity of these trends corresponded to the observation that many residues are fully conserved in TctA homologs and no residues are fully conserved in TctB homologs (15). It was predicted that TctA homologs have 11 or 12 TMSs while TctB homologs have four or infrequently five TMSs (15). Hydropathy analysis by the TMHMM, TopPred II, and SOSUI programs suggested that TctA and TpiA of E6 have 10 or 11 and 11 or 12 TMSs, respectively, and that TctB and TpiB have four and five TMSs, respectively. The 15-residue motif G-Hy_3-G-Hy_3-G-Hy_2-P-G-Hy-G (Hy, an aliphatic hydrophobic amino acid; fully conserved residues are underlined), well conserved in putative TMS 1 of TctA homologs (15), was also conserved in both TctA and TpiA (amino acids positions 26 to 40).

Disruption of *tctA* did not affect TPA uptake but resulted in complete losses of citrate uptake and growth on citrate (Fig. 3). These results indicate that *tctA* is essential for citrate uptake and suggest that *tctA* and *tctB* encode transmembrane proteins for the citrate transporter in E6. Similar to the gene encoding the TTT of citrate in *S.* Typhimurium, a putative citrate-binding protein gene, *tctC*, is located just upstream of *tctB* in E6. Moreover, the divergently transcribed *tctDE* genes, which encode a two-component regulatory system, were found immediately upstream of *tctC* (Fig. 2A). It is known that the TTT operon of *S.* Typhimurium is flanked by the genes encoding a putative two-component regulatory system (32). Recently, expression of the TTT genes involved in citrate uptake, *bctCBA*, in *Bordetella pertussis* was reported to be positively regulated in response to citrate by a two-component regulatory system, which consists of the BctE histidine kinase and the BctD response regulator (21). *bctE* and *bctD* are located just upstream of *bctC*. Based on the facts that citrate uptake by E6 cells was observed only in the cells grown on citrate and that the *tctDE* genes are present in the vicinity of *tctC*, expression of E6 *tctCBA* seems to be regulated by TctD and TctE. A gene set homologous to *tctDE* and *tctCBA* is conserved among the genomes of betaproteobacteria, including *C. testosteroni* CNB-2 (33), *C. testosteroni* S44 (34), *C. testosteroni* ATCC 11996 (35), *Delftia* sp. strain Cs1-4 (NC_015563), *C. testosteroni* KF-1 (NZ_AAUJ02000001), *Delftia acidovorans* SPH-1 (NC_010002), *Acidovorax* sp. strain KKS102 (36), *Acidovorax* sp. strain JS42 (NC_008782), *Acidovorax avenae* subsp. *avenae* ATCC 19860 (NC_015138), *Alicycliphilus denitrificans* BC (37), *Polaromonas naphthalenivorans* CJ2 (38), *Polaromo-*

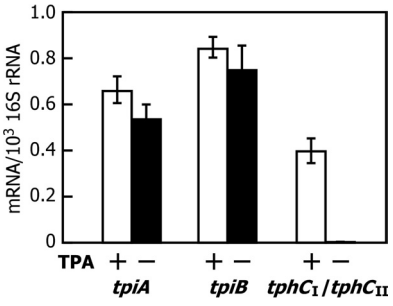

FIG 6 qRT-PCR analysis of the expression of *tpiA*, *tpiB*, and *tphC* in *Comamonas* sp. strain E6. Relative mRNA abundance was determined for *tpiA*, *tpiB*, and *tphC* ($tphC_I$ plus $tphC_{II}$). Total RNA was isolated from E6 cells grown in the presence (+) or absence (−) of 10 mM TPA. The data represent mRNA abundance normalized to 16S rRNA. Each value is the average ± standard deviation of three independent experiments.

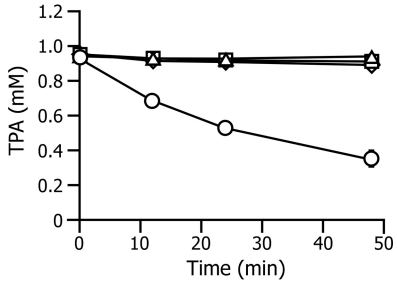

FIG 7 Conversion of TPA by the resting cells of *P. putida* PpY1100 carrying *tpiBA*, $tphC_{II}$, and $tphA2_{II}A3_{II}B_{II}A1_{II}$. TPA (1 mM) was incubated with resting PpY1100 cells harboring pJCBA ($tphC_{II}$ plus *tpiBA*; triangles), pJCtG ($tphC_{II}$ plus $tphA2_{II}A3_{II}B_{II}A1_{II}$; squares), pJBAtG (*tpiBA* plus $tphA2_{II}A3_{II}B_{II}A1_{II}$; diamonds), or pJCBAtG ($tphC_{II}$ plus *tpiBA* plus $tphA2_{II}A3_{II}B_{II}A1_{II}$; circles). The remaining TPA in the reaction mixture was periodically monitored by HPLC. Each value is the average ± standard deviation of three independent experiments.

nas sp. strain JS666 (39), *Leptothrix cholodnii* SP-6 (NC_010524), *Ramlibacter tataouinensis* TTB310 (40), and *Variovorax paradoxus* S110 (41). The *tctDE* and *tctCBA* genes appear to play a major role in citrate uptake in this group of betaproteobacteria.

RT-PCR and qRT-PCR analyses indicated that *tpiB* and *tpiA* are constitutively transcribed as a single operon (Fig. 6; see Fig. S5 in the supplemental material). Disruption of *tpiA* or *tpiB* resulted in complete loss of both the growth on TPA (Fig. 4; see Fig. S4) and TPA uptake (Fig. 5). These results suggest that *tpiA* and *tpiB* encode transmembrane proteins of the TPA transporter. In order to obtain clearer evidence, we carried out coexpression of *tpiBA* and $tphC_{II}$ with $tphA2_{II}A3_{II}B_{II}A1_{II}$ in *P. putida* PpY1100. Only when both $tphC_{II}$ and *tpiBA* were present in the PpY1100 cells together with $tphA2_{II}A3_{II}B_{II}A1_{II}$ were the resting cells of the transformant able to convert TPA (Fig. 7). These results strongly support the conclusion that the TPA transporter of E6 consists of the three components: the TPA-binding TphC, the large transmembrane protein TpiA, and the small transmembrane protein TpiB. It is noteworthy that successful expression of the TPA transporter genes with *tphA2A3BA1* in a heterologous host will support the establishment of bioprocesses for the conversion of TPA into industrially valuable intermediate metabolites, such as 2-pyrone-4,6-dicarboxylate, which is a building block for highly functional polymers (42–44).

In the genomes of the above-mentioned betaproteobacteria, which have *tctDE* and *tctCBA*, the highly similar gene set *tpiBA* is completely conserved even though only *C. testosteroni* CNB-2, *C. testosteroni* KF-1, and *R. tataouinensis* TTB310 have the *tph* gene cluster. This fact implies that *tpiBA* orthologs are involved in the uptake of solutes other than TPA in these bacteria. Disruption of *tpiA* or *tpiB* indeed caused the growth deficiency of E6 not only on TPA but also on IPA (Fig. 4; see Fig. S4 in the supplemental material). This fact strongly suggests that the TpiA-TpiB membrane components interact with at least TphC and the IPA-binding IphC. Furthermore, the growth of both *tpiA* and *tpiB* mutants on OPA and PCA was significantly retarded (Fig. 4; see Fig. S4). These results suggest that the TpiA-TpiB membrane components also interact with an unidentified OPA-binding protein and PCA-binding protein. Because the involvement of both an MFS transporter (OphD) and an ABC transporter (OphFGH) in OPA uptake by *Burkholderia* strains was demonstrated (8, 45), we searched the genome of *C. testosteroni* KF-1 for *ophD* and for putative SBP gene (*ophF*) orthologs. The product of CtesDRAFT_PD0442 revealed 44% identity with OphD; however, a similar ORF showing >30% identity at the amino acid sequence level with *ophF* was not found. E6 and KF-1 may employ both the TpiA-TpiB system and an MFS transporter to take up OPA. In regard to PCA uptake, we found an MFS transporter gene, *pmdK*, in the PCA 4,5-cleavage pathway operon, *pmdUKEFD ABC*, of E6 (31). The deduced amino acid sequence of E6 PmdK shows 47% identity with the PcaK transporter of 4-hydroxybenzoate/PCA in *P. putida* (2). Because the growth of the *pmdK* mutant of E6 on PCA was considerably delayed at neutral pH, both PmdK and the TpiA-TpiB system appear to be involved in PCA uptake. In addition, the rate of uptake of citrate by the *tpiA* mutant decreased to approximately 54% of the rate for the wild type, suggesting the involvement of the TpiA-TpiB system in citrate uptake. However, the reason why the *tctA* mutant lost the ability to take up citrate in spite of the existence of *tpiBA* remains unexplained at present.

It was documented that uptake by the TctCBA system is dependent on Na^+ and the membrane potential and is completely blocked by the addition of protonophores (15). Uptake of TPA by E6 cells in the absence of Na^+ was observed, and the addition of Na^+ did not enhance the uptake activity (data not shown). However, the protonophore CCCP completely inhibited TPA uptake, indicating that the TpiA-TpiB system is dependent on the proton motive force.

Uptake of [^{14}C]TPA by E6 cells was not inhibited by the presence of an excess amount of IPA, OPA, benzoate, 3-hydroxybenzoate, 4-hydroxybenzoate, vanillate, syringate, or citrate, suggesting that TphC strictly recognizes its proper substrate. On the other hand, uptake of [^{14}C]TPA by E6 cells was considerably inhibited in the presence of PCA. Because TPA is catabolized through PCA, expression of the genes involved in PCA catabolism, including the *pmd* operon, is induced in E6 cells when grown on TPA. One possible explanation for the inhibition of TPA uptake by PCA is that an unidentified gene encoding a PCA-binding protein was inducibly expressed in E6 cells grown on TPA and then the PCA-binding protein and TphC competed with each other for interactions with the TpiA-TpiB membrane components.

In this study, we identified and characterized a novel TTT-like system for TPA uptake in *Comamonas* sp. strain E6. This is the first report on the characterization of a TTT-like system involved in the uptake of aromatic acids. In addition, our results suggest for the first time that specific membrane components indeed interact with multiple SBPs of various substrates. While the *tctCBA* operon is specialized for citrate uptake in respect to substrate recognition and gene expression, the constitutive expression of *tpiBA* appears to be essential for multiple interactions of the TpiA-TpiB membrane components with various SBPs. However, further study will be necessary to uncover the actual involvement of the TpiA-TpiB system in the uptake of OPA, PCA, and citrate.

ACKNOWLEDGMENT

This work was supported by a Grant-in-Aid for Scientific Research (22580077) from the Japan Society for the Promotion of Science.

REFERENCES

1. **Pao SS, Paulsen IT, Saier MH, Jr.** 1998. Major facilitator superfamily. Microbiol. Mol. Biol. Rev. **62:**1–34.
2. **Nichols NN, Harwood CS.** 1997. PcaK, a high-affinity permease for the aromatic compounds 4-hydroxybenzoate and protocatechuate from *Pseudomonas putida*. J. Bacteriol. **179:**5056–5061.
3. **Leveau JH, Zehnder AJ, van der Meer JR.** 1998. The *tfdK* gene product facilitates uptake of 2,4-dichlorophenoxyacetate by *Ralstonia eutropha* JMP134(pJP4). J. Bacteriol. **180:**2237–2243.
4. **Collier LS, Nichols NN, Neidle EL.** 1997. *benK* encodes a hydrophobic permease-like protein involved in benzoate degradation by *Acinetobacter* sp. strain ADP1. J. Bacteriol. **179:**5943–5946.
5. **Xu Y, Wang SH, Chao HJ, Liu SJ, Zhou NY.** 2012. Biochemical and molecular characterization of the gentisate transporter GenK in *Corynebacterium glutamicum*. PLoS One **7:**e38701. doi:10.1371/journal.pone.0038701.
6. **Xu Y, Gao X, Wang SH, Liu H, Williams PA, Zhou NY.** 2012. MhbT is a specific transporter for 3-hydroxybenzoate uptake by Gram-negative bacteria. Appl. Environ. Microbiol. **78:**6113–6120.
7. **Davidson AL, Dassa E, Orelle C, Chen J.** 2008. Structure, function, and evolution of bacterial ATP-binding cassette systems. Microbiol. Mol. Biol. Rev. **72:**317–364.
8. **Chang HK, Dennis JJ, Zylstra GJ.** 2009. Involvement of two transport systems and a specific porin in the uptake of phthalate by *Burkholderia* spp. J. Bacteriol. **191:**4671–4673.
9. **Hara H, Stewart GR, Mohn WW.** 2010. Involvement of a novel ABC

transporter and monoalkyl phthalate ester hydrolase in phthalate ester catabolism by *Rhodococcus jostii* RHA1. Appl. Environ. Microbiol. **76:** 1516–1523.
10. **Arias-Barrau E, Sandoval A, Naharro G, Olivera ER, Luengo JM.** 2005. A two-component hydroxylase involved in the assimilation of 3-hydroxyphenyl acetate in *Pseudomonas putida*. J. Biol. Chem. **280:**26435–26447.
11. **Yuroff AS, Sabat G, Hickey WJ.** 2003. Transporter-mediated uptake of 2-chloro- and 2-hydroxybenzoate by *Pseudomonas huttiensis* strain D1. Appl. Environ. Microbiol. **69:**7401–7408.
12. **Allende JL, Gibello A, Fortún A, Mengs G, Ferrer E, Martín M.** 2000. 4-Hydroxybenzoate uptake in an isolated soil *Acinetobacter* sp. Curr. Microbiol. **40:**34–39.
13. **Allende JL, Gibello A, Martin M, Garrido-Pertierra A.** 1992. Transport of 4-hydroxyphenylacetic acid in *Klebsiella pneumoniae*. Arch. Biochem. Biophys. **292:**583–588.
14. **Mulligan C, Fischer M, Thomas GH.** 2011. Tripartite ATP-independent periplasmic (TRAP) transporters in bacteria and archaea. FEMS Microbiol. Rev. **35:**68–86.
15. **Winnen B, Hvorup RN, Saier MH, Jr.** 2003. The tripartite tricarboxylate transporter (TTT) family. Res. Microbiol. **154:**457–465.
16. **Chae JC, Zylstra GJ.** 2006. 4-Chlorobenzoate uptake in *Comamonas* sp. strain DJ-12 is mediated by a tripartite ATP-independent periplasmic transporter. J. Bacteriol. **188:**8407–8412.
17. **Sweet GD, Kay CM, Kay WW.** 1984. Tricarboxylate-binding proteins of *Salmonella typhimurium*. Purification, crystallization, and physical properties. J. Biol. Chem. **259:**1586–1592.
18. **Widenhorn KA, Boos W, Somers JM, Kay WW.** 1988. Cloning and properties of the *Salmonella typhimurium* tricarboxylate transport operon in *Escherichia coli*. J. Bacteriol. **170:**883–888.
19. **Widenhorn KA, Somers JM, Kay WW.** 1988. Expression of the divergent tricarboxylate transport operon (*tctI*) of *Salmonella typhimurium*. J. Bacteriol. **170:**3223–3227.
20. **Antoine R, Jacob-Dubuisson F, Drobecq H, Willery E, Lesjean S, Locht C.** 2003. Overrepresentation of a gene family encoding extracytoplasmic solute receptors in *Bordetella*. J. Bacteriol. **185:**1470–1474.
21. **Antoine R, Huvent I, Chemlal K, Deray I, Raze D, Locht C, Jacob-Dubuisson F.** 2005. The periplasmic binding protein of a tripartite tricarboxylate transporter is involved in signal transduction. J. Mol. Biol. **351:** 799–809.
22. **Huvent I, Belrhali H, Antoine R, Bompard C, Locht C, Jacob-Dubuisson F, Villeret V.** 2006. Crystal structure of *Bordetella pertussis* BugD solute receptor unveils the basis of ligand binding in a new family of periplasmic binding proteins. J. Mol. Biol. **356:**1014–1026.
23. **Sasoh M, Masai E, Ishibashi S, Hara H, Kamimura N, Miyauchi K, Fukuda M.** 2006. Characterization of the terephthalate degradation genes of *Comamonas* sp. strain E6. Appl. Environ. Microbiol. **72:**1825–1832.
24. **Fukuhara Y, Inakazu K, Kodama N, Kamimura N, Kasai D, Katayama Y, Fukuda M, Masai E.** 2010. Characterization of the isophthalate degradation genes of *Comamonas* sp. strain E6. Appl. Environ. Microbiol. **76:**519–527.
25. **Antoine R, Raze D, Locht C.** 2000. Genomics of *Bordetella pertussis* toxins. Int. J. Med. Microbiol. **290:**301–305.
26. **Kasai D, Kamimura N, Tani K, Umeda S, Abe T, Fukuda M, Masai E.** 2012. Characterization of FerC, a MarR-type transcriptional regulator, involved in transcriptional regulation of the ferulate catabolic operon in *Sphingobium* sp. strain SYK-6. FEMS Microbiol. Lett. **332:**68–75.
27. **Krogh A, Larsson B, von Heijne G, Sonnhammer EL.** 2001. Predicting transmembrane protein topology with a hidden Markov model: application to complete genomes. J. Mol. Biol. **305:**567–580.
28. **Claros MG, von Heijne G.** 1994. TopPred II: an improved software for membrane protein structure predictions. Comput. Appl. Biosci. **10:**685–686.
29. **Hirokawa T, Boon-Chieng S, Mitaku S.** 1998. SOSUI: classification and secondary structure prediction system for membrane proteins. Bioinformatics **14:**378–379.
30. **Sato Y, Moriuchi H, Hishiyama S, Otsuka Y, Oshima K, Kasai D, Nakamura M, Ohara S, Katayama Y, Fukuda M, Masai E.** 2009. Identification of three alcohol dehydrogenase genes involved in the stereospecific catabolism of arylglycerol-β-aryl ether by *Sphingobium* sp. strain SYK-6. Appl. Environ. Microbiol. **75:**5195–5201.
31. **Kamimura N, Aoyama T, Yoshida R, Takahashi K, Kasai D, Abe T, Mase K, Katayama Y, Fukuda M, Masai E.** 2010. Characterization of the protocatechuate 4,5-cleavage pathway operon in *Comamonas* sp. strain E6 and discovery of a novel pathway gene. Appl. Environ. Microbiol. **76:** 8093–8101.
32. **Widenhorn KA, Somers JM, Kay WW.** 1989. Genetic regulation of the tricarboxylate transport operon (*tctI*) of *Salmonella typhimurium*. J. Bacteriol. **171:**4436–4441.
33. **Ma YF, Zhang Y, Zhang JY, Chen DW, Zhu Y, Zheng H, Wang SY, Jiang CY, Zhao GP, Liu SJ.** 2009. The complete genome of *Comamonas testosteroni* reveals its genetic adaptations to changing environments. Appl. Environ. Microbiol. **75:**6812–6819.
34. **Xiong J, Li D, Li H, He M, Miller SJ, Yu L, Rensing C, Wang G.** 2011. Genome analysis and characterization of zinc efflux systems of a highly zinc-resistant bacterium, *Comamonas testosteroni* S44. Res. Microbiol. **162:**671–679.
35. **Gong W, Kisiela M, Schilhabel MB, Xiong G, Maser E.** 2012. Genome sequence of *Comamonas testosteroni* ATCC 11996, a representative strain involved in steroid degradation. J. Bacteriol. **194:**1633–1634.
36. **Ohtsubo Y, Maruyama F, Mitsui H, Nagata Y, Tsuda M.** 2012. Complete genome sequence of *Acidovorax* sp. strain KKS102, a polychlorinated-biphenyl degrader. J. Bacteriol. **194:**6970–6971.
37. **Oosterkamp MJ, Veuskens T, Plugge CM, Langenhoff AA, Gerritse J, van Berkel WJ, Pieper DH, Junca H, Goodwin LA, Daligault HE, Bruce DC, Detter JC, Tapia R, Han CS, Land ML, Hauser LJ, Smidt H, Stams AJ.** 2011. Genome sequences of *Alicycliphilus denitrificans* strains BC and K601T. J. Bacteriol. **193:**5028–5029.
38. **Yagi JM, Sims D, Brettin T, Bruce D, Madsen EL.** 2009. The genome of *Polaromonas naphthalenivorans* strain CJ2, isolated from coal tar-contaminated sediment, reveals physiological and metabolic versatility and evolution through extensive horizontal gene transfer. Environ. Microbiol. **11:**2253–2270.
39. **Mattes TE, Alexander AK, Richardson PM, Munk AC, Han CS, Stothard P, Coleman NV.** 2008. The genome of *Polaromonas* sp. strain JS666: insights into the evolution of a hydrocarbon- and xenobiotic-degrading bacterium, and features of relevance to biotechnology. Appl. Environ. Microbiol. **74:**6405–6416.
40. **De Luca G, Barakat M, Ortet P, Fochesato S, Jourlin-Castelli C, Ansaldi M, Py B, Fichant G, Coutinho PM, Voulhoux R, Bastien O, Marechal E, Henrissat B, Quentin Y, Noirot P, Filloux A, Mejean V, DuBow MS, Barras F, Barbe V, Weissenbach J, Mihalcescu I, Vermeglio A, Achouak W, Heulin T.** 2011. The cyst-dividing bacterium *Ramlibacter tataouinensis* TTB310 genome reveals a well-stocked toolbox for adaptation to a desert environment. PLoS One **6:**e23784. doi:10.1371/journal.pone.0023784.
41. **Han JI, Choi HK, Lee SW, Orwin PM, Kim J, Laroe SL, Kim TG, O'Neil J, Leadbetter JR, Lee SY, Hur CG, Spain JC, Ovchinnikova G, Goodwin L, Han C.** 2011. Complete genome sequence of the metabolically versatile plant growth-promoting endophyte *Variovorax paradoxus* S110. J. Bacteriol. **193:**1183–1190.
42. **Michinobu T, Bito M, Yamada Y, Katayama Y, Noguchi K, Masai E, Nakamura M, Ohara S, Shigehara K.** 2007. Molecular properties of 2-pyrone-4,6-dicarboxylic acid (PDC) as a stable metabolic intermediate of lignin isolated by fractional precipitation with Na^+ ion. Bull. Chem. Soc. Jpn. **80:**2436–2442.
43. **Michinobu T, Hishida M, Sato M, Katayama Y, Masai E, Nakamura M, Otsuka Y, Ohara S, Shigehara K.** 2008. Polyesters of 2-pyrone-4,6-dicarboxylic acid (PDC) obtained from a metabolic intermediate of lignin. Polym. J. **40:**68–75.
44. **Michinobu T, Bito M, Yamada Y, Tanimura M, Katayama Y, Masai E, Nakamura M, Otsuka Y, Ohara S, Shigehara K.** 2009. Fusible, elastic, and biodegradable polyesters of 2-pyrone-4,6-dicarboxylic acid (PDC). Polym. J. **41:**1111–1116.
45. **Chang HK, Zylstra GJ.** 1999. Characterization of the phthalate permease OphD from *Burkholderia cepacia* ATCC 17616. J. Bacteriol. **181:**6197–6199.